APPLIED SCIENCES AND ENGINEERING

Attenuated diphtheria toxin mediates siRNA delivery

Amy E. Arnold[1], Laura J. Smith[2,3], Greg L. Beilhartz[4], Laura C. Bahlmann[3], Emma Jameson[2], Roman A. Melnyk[4,5], Molly S. Shoichet[1,2,3]*

Toxins efficiently deliver cargo to cells by binding to cell surface ligands, initiating endocytosis, and escaping the endolysosomal pathway into the cytoplasm. We took advantage of this delivery pathway by conjugating an attenuated diphtheria toxin to siRNA, thereby achieving gene downregulation in patient-derived glioblastoma cells. We delivered siRNA against integrin-β1 (*ITGB1*)—a gene that promotes invasion and metastasis—and siRNA against eukaryotic translation initiation factor 3 subunit b (*eIF-3b*)—a survival gene. We demonstrated mRNA downregulation of both genes and the corresponding functional outcomes: knockdown of *ITGB1* led to a significant inhibition of invasion, shown with an innovative 3D hydrogel model; and knockdown of *eIF-3b* resulted in significant cell death. This is the first example of diphtheria toxin being used to deliver siRNAs, and the first time a toxin-based siRNA delivery strategy has been shown to induce relevant genotypic and phenotypic effects in cancer cells.

INTRODUCTION

Pathogens produced by bacteria have evolved over millions of years to achieve highly sophisticated mechanisms of penetrating cells, responding to intracellular cues to guide their trafficking, and to deliver their payload to a desired site of action. In particular, "AB"-type toxins, such as anthrax toxin (AT) and diphtheria toxin (DT), bind to the cell surface, are endocytosed, escape the endosomal pathway, and translocate into the cytosol (*1*). These toxins are made up of three domains: an active (toxic) domain, "A," that can be mutated to attenuate its toxicity for delivery applications (i.e., "*a*") (*2*); a translocation domain, "T," that facilitates escape from the endosomes; and a receptor binding domain, "R," that binds a receptor on the cell surface for targeting and inducing endocytosis (Fig. 1A) (*3*). Together, the T and R domains are referred to as one "B" subunit that brings the A domain into cells, hence the terminology AB toxins. Taking advantage of the cell entry mechanism of AB toxins through cargo-toxin fusion constructs has been explored for delivery of diverse protein cargos including peptides, effector proteins, and antibody-like proteins (*2*, *4*). There has been only one example of oligonucleotide delivery with attenuated AT reported; however, this preliminary study did not demonstrate any functional effects of gene knockdown (*5*).

Oligonucleotides, such as small interfering RNAs (siRNAs), are powerful tools to regulate gene expression in diseased cells, with the potential to return them to a normal phenotype (*6*). However, therapeutic siRNA delivery represents a significant clinical challenge because of the many physiological barriers that must be overcome for efficacy, as well as the toxicity and immunogenicity of many currently used delivery vehicles (*7*, *8*). Commonly, siRNAs are delivered via liposomal or polymeric nanoparticle formulations, which are reviewed extensively elsewhere (*9*). One of the biggest barriers to siRNA delivery is entrapment in the endolysosomal pathway after endocytosis, quickly leading to degradation of the fragile, nuclease-prone siRNA (*10*). Strategies that enhance the endosomal escape of siRNA have recently attracted much attention (*11*, *12*). Many of these strategies use liposomal formulations for the delivery of siRNA; however, the biodistribution of these nanoparticles is largely limited to clearance organs such as the liver and kidney (*13*). To overcome biodistribution challenges, targeting proteins such as antibodies have been explored to deliver siRNAs to specific tissues with some success (*14*, *15*); however, only a very small percentage of antibody-siRNA conjugates escape the endosomal pathway, limiting their efficacy (*16*). AB toxins, such as DT, have the capacity for both endosomal escape and specific targeting (*17*) and are thus attractive candidates for siRNA delivery into the cytoplasm (Fig. 1B).

We explored whether attenuated DT (*a*DT) could be used as a delivery vehicle for siRNAs against two cancer gene targets: (i) *eIF-3b*, a transcription factor that is overexpressed in many cancers and the inhibition of which slows growth and initiates apoptosis (*18*), and (ii) *ITGB1*, which is involved in the formation of focal adhesions and activation of actin rearrangement, the inhibition of which reduces cellular invasion and metastasis (*19*). We chose to focus on the delivery of siRNA to glioblastoma (GBM) cells, and specifically GBM stem cell (GSC)–enriched cultures, because of the following: (i) DT has been reported to cross the blood brain barrier, making it an attractive vehicle against intractable diseases like GBM (*20*); however, this has yet to be tested with a DT-siRNA conjugate. (ii) The DT receptor, heparin-binding epidermal growth factor (HBEGF), is widely expressed in the central nervous system (*21*) and is overexpressed in at least a subset of malignant gliomas (*22*). (iii) There is a growing body of evidence that the aggressiveness of GBM is, at least in part, caused by the GSC subpopulation (*23*). (iv) The GSCs are rapidly dividing and highly invasive (*24*), allowing functional readouts for both cell viability and invasiveness. For the purposes of these studies, we chose to use Dicer-substrate siRNAs, 27-mer siRNAs that are processed by the Dicer enzyme within the cell and are typically more potent than the standard 21- to 23-mer siRNA equivalent (*25*).

We conjugated an engineered *a*DT to Dicer-substrate siRNAs against *eIF-3b* and *ITGB1* using azide-alkyne click chemistry. There are many conjugation strategies available to conjugate cargo to proteins; however, the essential disulfide bond linking the A and T domains of DT precluded the use of reducing agents during synthesis

[1]Department of Chemistry, University of Toronto, Toronto, ON, Canada. [2]Department of Chemical Engineering and Applied Chemistry, University of Toronto, Toronto, ON, Canada. [3]Institute of Biomaterials and Biomedical Engineering, University of Toronto, Toronto, ON, Canada. [4]Program in Molecular Medicine, The Hospital for Sick Children, Toronto, ON, Canada. [5]Department of Biochemistry, University of Toronto, Toronto, ON, Canada.
*Corresponding author. Email: molly.shoichet@utoronto.ca

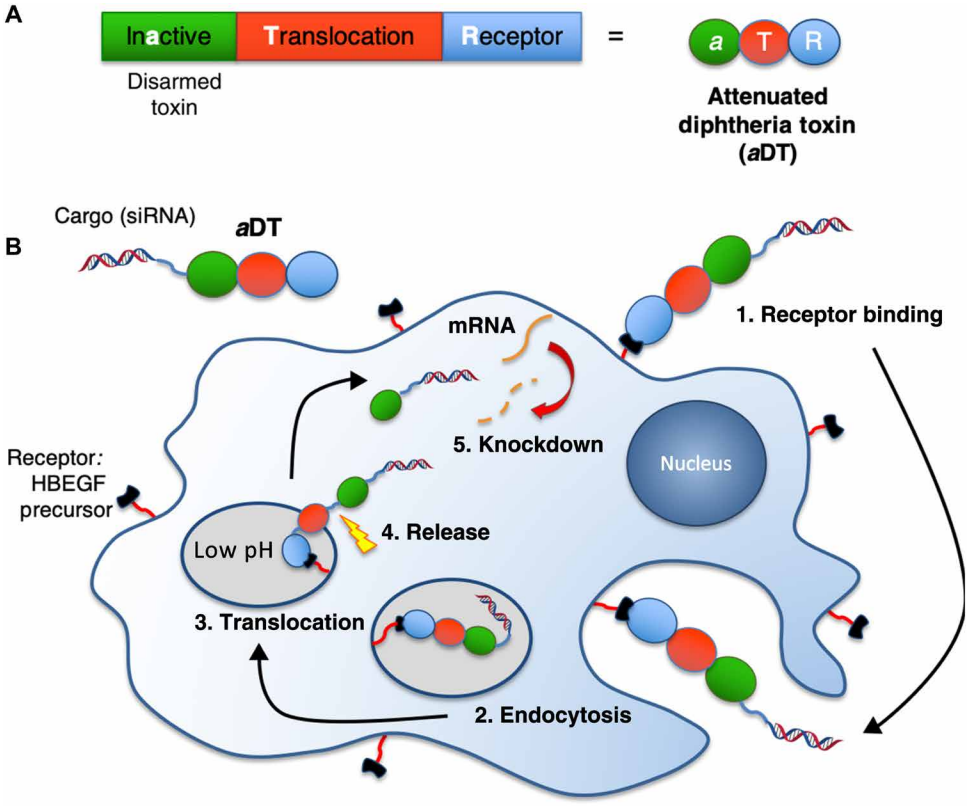

Fig. 1. Using *a*DT for siRNA delivery. (**A**) Attenuated AB toxins, such as attenuated DT (*a*DT), consist of three main components: a receptor binding domain (R) that binds to a receptor on the cell surface, a translocation domain (T) that allows for endosomal escape, and a mutated active domain (*a*) for the protein to retain its trafficking functions but be no longer toxic to cells. Cargo, such as small interfering RNA (siRNA), can be attached to this *a* domain. (**B**) siRNA delivered using *a*DT occurs in five main steps: (1) binding to the heparin-binding epidermal growth factor (HBEGF) precursor cell surface receptor; (2) endocytosis of the *a*DT-siRNA cargo; (3) translocation through the endosomal membrane, inserting the *a* domain and cargo into the cytoplasm; (4) cleavage of the *a* domain from the rest of the protein; and (5) release of the siRNA into the cytoplasm where it down-regulates the relevant gene.

of the *a*DT-siRNA conjugate (*26*). The click chemistry approach that we used was efficient, bio-orthogonal, produced no by-products (*27*), and maintained the integrity of the rest of the protein by avoiding the use of reducing agents. We examined the biological effects of these conjugates by measuring mRNA expression levels, assessed cell viability and invasiveness, and thus demonstrate this platform strategy in vitro with both gene knockdown and functional assays in primary human GBM cells.

RESULTS

Conjugation of siRNA to *a*DT

For *a*DT-mediated siRNA delivery, we used an engineered *a*DT containing a cysteine for chemical modification, a SUMO tag for increased stability, and a His tag for purification (Fig. 2A). We modified this *a*DT-cysteine variant with a maleimide-modified cross-linker containing a dibenzocyclooctyne (DBCO) as a handle for further chemical modification (Fig. 2B). Successful synthesis of *a*DT-DBCO was demonstrated by absorbance, with clear peaks at 280 nm (representing the DT) and 309 nm (representing the DBCO). The peak at 309 nm was absent in *a*DT alone (Fig. 2C). We then reacted Dicer-substrate siRNA containing an azide functionality at the 3′-end of the sense strand with the *a*DT-DBCO to form the *a*DT-siRNA conjugate (Fig. 2D). Previous studies have shown that conjugation of Dicer-substrate siRNAs through the 3′-end of the sense strand leads to more potent gene suppression than conjugation at the 5′-end of the sense strand or either terminus of the antisense strand (*28*). High (5 to 10) equivalents of the siRNA were required to obtain an adequate (~50%) conjugation efficiency at 37°C (fig. S1). However, we found that we could achieve 55% conjugation of *a*DT to siRNA with only one equivalent of siRNA by adapting a method by Takemoto *et al.* (*29*) wherein the *a*DT-siRNA mixture was incubated for 1 hour at room temperature, frozen at −20°C, and then thawed for 1 hour at 4°C (Fig. 2E). We purified the *a*DT-siRNA by conjugating it to nickel beads via the His tag on the *a*DT and washing away the excess siRNA, with only a small amount (~15%) of unbound siRNA remaining (Fig. 2F). The *a*DT-siRNA demonstrated similar stability to siRNA against serum nucleases (fig. S2), which would be encountered both in the extracellular environment and inside the endolysosomal pathway.

GSCs express HBEGF

The GSCs used in this study were patient-derived GBM cells grown under stem cell conditions, as previously described (*30*). We verified that *a*DT was a good candidate for targeting and internalization in GSCs by both staining the cells for the DT receptor, HBEGF, which was abundantly evident (green staining in Fig. 3), and measuring the half maximal inhibitory concentration (IC_{50}) of the wild-type (toxic)

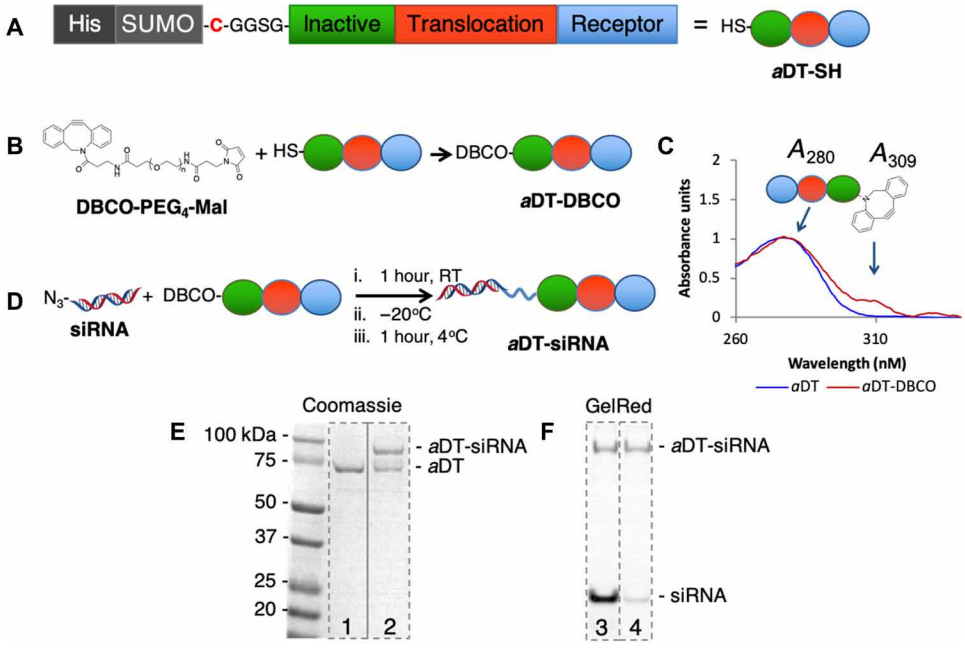

Fig. 2. siRNAs can be conjugated to *a*DT. (**A**) *a*DT was engineered to contain a free cysteine as a functional handle (*a*DT-SH), protected by a SUMO tag and purified using a histidine (His) tag. (**B**) *a*DT was reacted with a PEG cross-linker containing both maleimide and DBCO functional groups to obtain DBCO-modified *a*DT (*a*DT-DBCO). (**C**) The presence of the DBCO modification on *a*DT was confirmed by measuring the absorbance at 280 nm (*a*DT) and 309 nm (DBCO). Curves shown are *a*DT before modification (blue) and after DBCO modification (red). A_{280}, absorbance at 280 nm. (**D**) Azide-modified siRNA was reacted with the DBCO-functionalized *a*DT to obtain the *a*DT-siRNA conjugate. RT, room temperature. (**E**) Modification of the *a*DT with the siRNA was confirmed via polyacrylamide gel electrophoresis (PAGE) stained with Coomassie blue to localize the DT protein. Lane 1 shows the *a*DT-DBCO starting material (M_w, ~72,000), and lane 2 shows the *a*DT-siRNA conjugate (M_w, ~90,000) alone with some unreacted starting material. (**F**) Purification of the excess siRNA was confirmed via PAGE stained with GelRed to localize the siRNA. Lane 3 shows the *a*DT-siRNA conjugate along with unreacted siRNA; lane 4 shows the *a*DT-siRNA conjugate after nickel column purification, with only a small amount of excess siRNA left over.

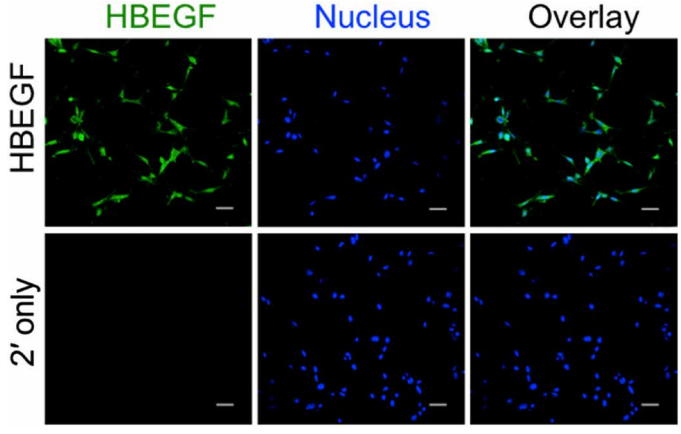

Fig. 3. GSCs express HBEGF, the native receptor for DT. Representative confocal images are shown for HBEGF (anti-HBEGF antibody; green) and nucleus (Hoechst; blue). The secondary antibody–only control confirms lack of nonspecific binding. Scale bars, 50 μm.

DT against these cells to ensure the correct mechanism of action. The IC_{50} of the wild-type DT in the GSCs was 6.0 ± 1.0 pM (fig. S3A), indicating high sensitivity to the toxin and a conserved internalization and translocation mechanism therein. We confirmed that the sensitivity of GBM cells to the DT could be generalized to other GBM cell lines (fig. S3B). All further experiments were conducted with a non–wild-type *a*DT with an insignificant level of toxicity as previously reported (*2*).

*a*DT-siRNA conjugate down-regulates *ITGB1* and reduces cellular invasion

We conjugated *a*DT to Dicer-substrate siRNA against two relevant gene targets: *ITGB1* (to make *a*DT-ITGB1) and *eIF-3b* (to make *a*DT–eIF-3b). We treated the GSCs with the *a*DT-ITGB1 conjugate and observed a significant reduction in the target mRNA compared to negative controls of siRNA only (without Lipofectamine) and *a*DT conjugated to a nontargeting siRNA (*a*DT-NT) at 50 nM (Fig. 4A). siRNA-only negative control indicates that delivery to the cells is mediated by the DT via the HBEGF receptor and that the small amount of unbound siRNA in the system is not affecting gene knockdown. To ascertain whether the reduction in *ITGB1* expression would correspond to a phenotype of either reduced invasion or adhesion, we seeded the cells on top of a cross-linked hyaluronic acid–based three-dimensional (3D) hydrogel, which the cells normally invade (Fig. 4B) (*31*). Impressively, we observed a notable decrease in invasiveness in *a*DT-ITGB1–treated cells compared to untreated or *a*DT-NT controls (Fig. 4, C and D). To determine whether cell adhesion influenced these results, we pretreated the cells cultured in 2D tissue culture polystyrene flasks with both *a*DT-ITGB1 and *a*DT-NT before plating them on the 3D hydrogels. After several wash steps, we observed no significant difference in the number of adhered cells between any of the treatment groups, demonstrating that cell adhesion did not

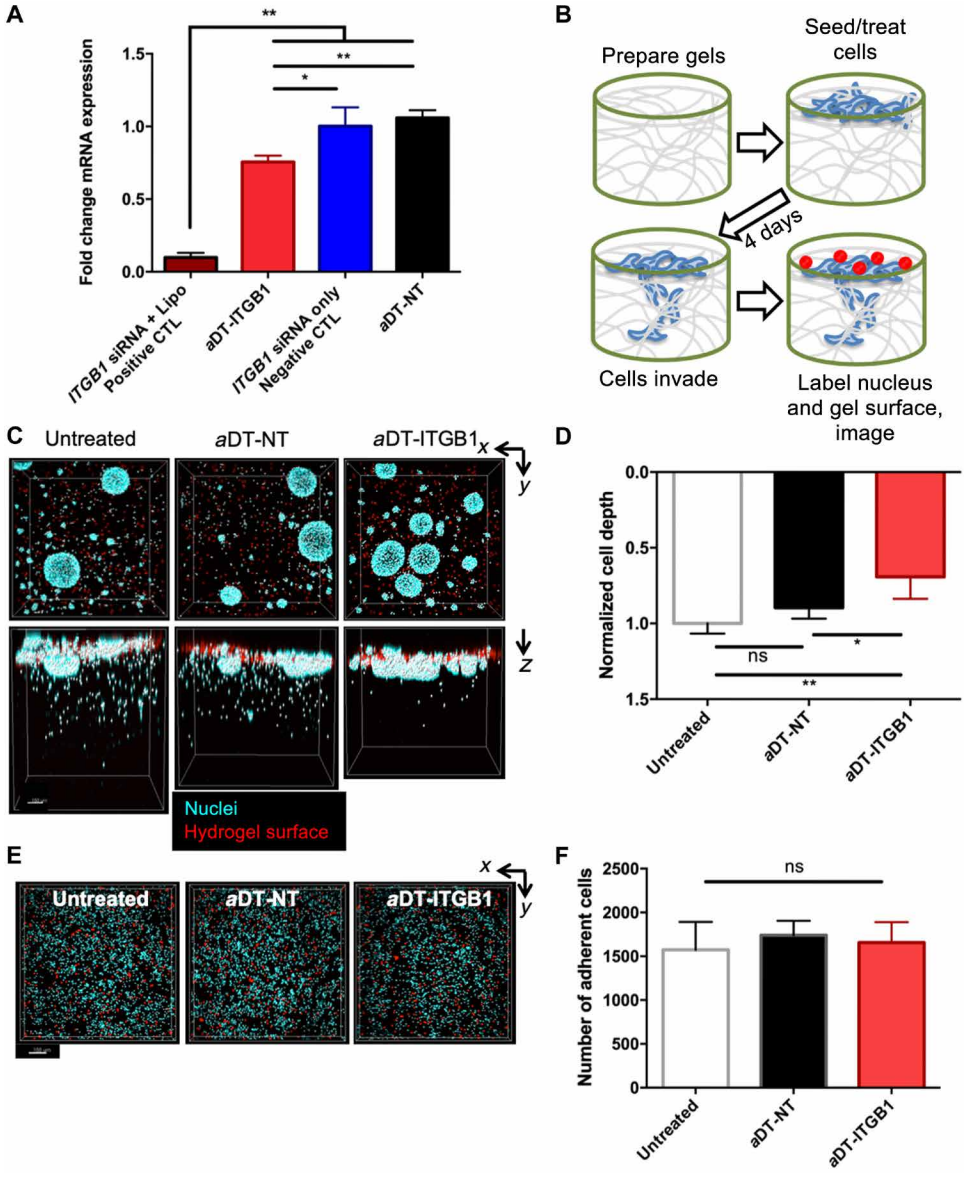

Fig. 4. *a*DT-siRNA down-regulates *ITGB1* expression in GSCs and reduces cellular invasion. (**A**) *a*DT-ITGB1 (light red bars) down-regulates *ITGB1* mRNA expression compared to negative controls (CTL): *a*DT-NT (black bars) and *ITGB1* siRNA only without Lipofectamine (blue bar) at 24 hours after treatment. Positive control is transfected *ITGB1* siRNA with Lipofectamine (dark red bar). Data are shown as $n = 3$, are means ± SD, and are normalized to an untreated control. Data were analyzed using one-way analysis of variance (ANOVA), followed by Tukey's correction on the logarithmic data (*$P < 0.05$ and **$P < 0.01$). (**B**) Cells were plated in a 3D hydrogel assay on the surface of preformed hydrogels and treated with *a*DT-ITGB1 conjugates at the beginning of the experiment. Invasion depth was measured after 5 days. (**C**) *a*DT-ITGB1 reduces invasion compared to controls (no treatment and *a*DT-NT) in a 3D hydrogel model. Representative images are shown. Fifteen-micrometer red beads label the top of the hydrogel; blue cell nuclei are labeled using Hoechst. Scale bar, 50 μm. (**D**) Invasion depth was quantified as a percentage of the untreated control. Data were analyzed using one-way ANOVA, followed by Tukey's correction (*$P < 0.05$ and **$P < 0.01$). ns, not significant. (**E**) *a*DT-ITGB1 did not reduce the number of adhered cells in a 3D hydrogel model. Representative images are shown. Scale bar, 150 μm. (**F**) Number of adherent cells was quantified by counting the number of cell nuclei; no significant difference was observed, demonstrating that differences in invasion were due to *ITGB1* down-regulation. Data were analyzed using one-way ANOVA, followed by Tukey's correction.

affect the reduced cell invasion observed with *a*DT-ITGB1 treatment (Fig. 4, E and F).

*a*DT-siRNA conjugate down-regulates *eIF-3b* and reduces cell viability

*a*DT–eIF-3b–treated GBM cells exhibited significant down-regulation in the target mRNA compared to the relevant negative controls of siRNA only (without Lipofectamine) and *a*DT-NT at 50 nM (Fig. 5A). We confirmed that the *eIF-3b* siRNA could reduce cell viability in the GSCs by complexing *eIF-3b* siRNA and NT siRNA with a commercially available transfection reagent and observing a significant difference in cell viability with *eIF-3b* siRNA–mediated knockdown (fig. S4). Furthermore, we observed a significant (albeit modest) reduction of cell viability with an *a*DT–eIF-3b concentration of 100 nM (Fig. 5B). These data also demonstrate that *a*DT (as *a*DT-NT) is nontoxic at a concentration of up to 100 nM (Fig. 5B). A competition

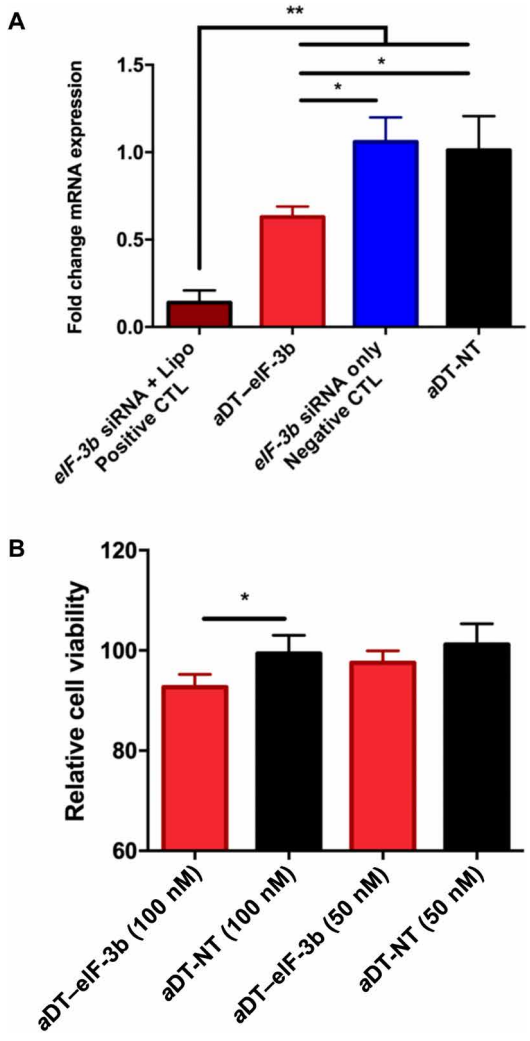

Fig. 5. *a*DT-siRNA down-regulates *eIF-3b* expression in GSCs and reduces cell viability. (**A**) *a*DT–eIF-3b (light red bar) down-regulates *eIF-3b* mRNA expression compared to negative controls: *a*DT-NT (black bar) and *eIF-3b* siRNA only without Lipofectamine (blue bar) at 24 hours after treatment. Positive control is transfected siRNA with Lipofectamine (dark red bar). Data are shown as $n = 3$, are means ± SD, and are normalized to an untreated control. Data were analyzed using one-way ANOVA, followed by Tukey's correction on the logarithmic data (*$P < 0.05$ and **$P < 0.01$). (**B**) *a*DT–eIF-3b (red bars) reduces cell viability of GSCs at 48 hours after treatment compared to *a*DT-NT (black bars) at 100 nM. Data are shown as $n = 3$, are means + SD, and are normalized to an untreated control. Data were analyzed using one-way ANOVA, followed by Sidak's correction (*$P < 0.05$).

assay with cells treated with a 10× excess of *a*DT further confirmed that delivery is mediated by *a*DT via the HBEGF receptor (fig. S5).

DISCUSSION

We show the first example of siRNA delivery mediated by DT. Exploiting the sophisticated trafficking mechanism of proteins, such as that of *a*DT, has the potential to overcome many of the barriers to siRNA delivery. Using our *a*DT-siRNA conjugate, we were able to down-regulate two distinct genetic targets and observe significant changes in cell proliferation and invasion, supporting the robust nature of *a*DT-mediated drug delivery and its potential as a previously unidentified treatment strategy for aggressive cancers such as GBM. *a*DT is an advantageous siRNA delivery vehicle for GBM treatment for two main reasons: (i) targeting via the receptor binding domain and (ii) endosomal escape via the translocation domain. HBEGF proved to be a good target for siRNA delivery, as it is expressed in the GSCs that are used in this study and is widely expressed in brain tissue (*21*). It is essential to develop strategies that can target the GSCs in addition to the bulk tumor, as GSCs may be responsible for tumor recurrence (*32*).

Endosomal escape is important for the delivery of siRNAs to avoid trafficking into the late endosomes/lysosomes and subsequent degradation by nucleases (*33*). *a*DT has been reported to translocate out of the endolysosomal pathway at a relatively early endosomal stage (pH, ~6.5), protecting its cargo from the harsh degradation environment of the lysosomes (*34*). The *a*DT and its cargo translocate through a flexible α-helical pore (*2*), making endosomal escape difficult to assay directly because most current methods measure widespread membrane leakage (*35*). However, the gene knockdown and subsequent phenotypic effects of siRNA delivery that we observed confirmed successful *a*DT-mediated translocation, as previous work has shown that without translocation and endosomal escape, the *a*DT cannot deliver cargo (*2*). We confirmed the robust nature of the *a*DT-siRNA system by down-regulating two genes of interest in the target cells. In comparison, in systems that do not have inherent endosomal escape capabilities, such as antibody-siRNA conjugates, delivery has been shown to be highly target dependent (*16*). While AT was used for siRNA delivery previously, knockdown of only a proof-of-concept target was shown without downstream functional effects (*5*). Using our *a*DT conjugate system, we observed phenotypic changes in both cell invasion and growth.

Diffuse tumor cell infiltration is a hallmark of GBM, and recent findings have suggested that GSCs play important roles in migration and invasion (*24*). It has been reported that inhibiting GSC invasion is essential to slowing the progression of GBM (*36*). *ITGB1* is involved in cellular binding to many extracellular matrix components, including fibronectin (*37*), and *ITGB1* knockdown has been shown to reduce invasion in cancer cells (*38*). Thus, we hypothesized that *ITGB1* knockdown would reduce the invasive behavior of GSCs. We demonstrated the effectiveness of the *a*DT-ITGB1 conjugate in reducing cell invasion using a previously validated 3D hydrogel platform (*31*), confirming a functional effect of siRNA-mediated knockdown. Moreover, as GSCs have also been shown to drive tumor growth (*39*), we were also interested in using our treatment strategy to reduce cellular proliferation. We used an siRNA targeted against *eIF-3b*, which is known to reduce protein synthesis, leading to a reduction in cell growth and viability (*40*). Using the *a*DT–eIF-3b conjugate, we successfully reduced *eIF-3b* expression and observed a corresponding change in cell viability. Thus, we demonstrated functional effects of gene knockdown in two different pathways, indicating that this *a*DT-siRNA can be considered a platform strategy.

We demonstrated a robust platform for siRNA delivery to GSCs using an *a*DT as a delivery vehicle with an inherent endosomal escape mechanism. In future work, this conjugate will be used for siRNA delivery in vivo to orthotopic models of GBM from multiple patient-derived cell strains. Potential in vivo study designs would compare intracranial injection to intravenous delivery while using chemically stabilized siRNAs to avoid nuclease degradation (*41*). A major outcome of this in vivo study would be determining the ability of the *a*DT-siRNA conjugate to cross the blood brain barrier and diffuse

into the brain tissue. We expect the protein conjugate to diffuse some distance into the brain tissue based on previous studies (*42*). Further extensions of this work could include combination with chemotherapeutics, or altering the receptor binding domain to bind to other targets (*43*, *44*), to develop innovative treatments for a broad range of cancers and other diseases.

MATERIALS AND METHODS

Cell lines

Patient-derived glioma neural stem cells (GNS 411) were a gift from the laboratory of P. Dirks, with Research Ethics Board approval at the Hospital for Sick Children, Toronto and the University of Toronto. The characterization of these cells as GSC-enriched cultures is presented in several publications by Park *et al*. and Dolma *et al.* (*45*, *46*). These cells are referred to as GSCs throughout the manuscript. Cells were maintained in an incubator (37°C, 5% CO_2, and 95% humidity) grown in Corning Primaria flasks (Corning, 353808) coated with poly-L-ornithine (PLO; Sigma-Aldrich, P4957) and laminin (Sigma-Aldrich, 11243217001). GSC growth media contained serum-free NeuroCult NS-A Basal Medium (STEMCELL Technologies, 05750) supplemented with N2, B27, EGF, fibroblast growth factor, and heparin as previously described for neural stem cells (*47*).

Attenuated DT

*a*DT was expressed as previously described (*2*). Briefly, *a*DT was expressed in *Escherichia coli* BL21(DE3) cells, induced with 1 mM isopropyl-β-D-1-thiogalactopyranoside for 4 hours at 37°C using the Champion pET SUMO Expression System (Invitrogen). Cells were harvested by centrifugation, resuspended in lysis buffer [20 mM tris-HCl (pH 8.0), 0.5 M NaCl, 20 mM imidazole, Benzonase, lysozyme, and protease inhibitor cocktail], and lysed by an EmulsiFlex C3 microfluidizer (Avestin) at 15,000 psi. The lysates were centrifuged at 18,000*g* for 20 min. The His-tagged DT was purified by nickel affinity chromatography using a HisTrap FF column (GE Healthcare).

siRNAs

Dicer-substrate siRNAs were purchased as annealed duplexes from Integrated DNA Technologies. All siRNAs were suspended at a concentration of ~50 nM using nuclease-free duplex buffer (Dharmacon, B-002000-UB-100). Concentrations were verified by measuring the absorbance at 260 nm. Sequences of Dicer-substrate siRNAs used were as follows: *eIF-3b* sense, 5′-rGrG rArUrA rCrGrC rUrUrA rGrCrA rUrCrU rArUrG rArArA CT-azide-3′; *eIF-3b* antisense, 5′-rArG rUrUrU rCrArU rArGrA rUrGrC rUrArA rGrCrG rUrArU rCrCrA rG-3′; *ITGB1* sense, 5′-rGrA rCrUrG rUrUrC rUrUrU rGrGrA rUrArC rUrArG rUrArC TT-azide-3′; and *ITGB1* antisense, rArA rGrUrA rCrUrA rGrUrA rUrCrC rArArA rGrArA rCrArG rUrCrA rC-3′.

Polymerase chain reaction primers

Primers used were purchased from ACGT Corp. for *eIF-3b* (*48*) (forward, 5′-TGTGAAAGGTACCTGGTGAC-3′ and reverse, 5′-AATAGGCCAATGGGCTGAG-3′) and ITGB1 (*49*) (forward, 5′-GAAAACAGCGCATATCTGGAAATT-3′ and reverse, 5′-CAGCCAATCAGTGATCCACAA-3′).

Immunocytochemistry (HBEGF)

GSCs were plated to reach 60 to 80% confluency on chambered cover glass slides coated with PLO and laminin. Cells were then fixed with 4% paraformaldehyde (PFA) and stained using an antibody specific for HBEGF (Abcam, ab66792), followed by a fluorescently labeled secondary antibody (Thermo Fisher Scientific, A-11001). The cells were then counterstained with Hoechst 33342, and images were captured on an Olympus FV1000 confocal microscope.

Preparation of *a*DT-siRNA conjugate

*a*DT was modified with a DBCO-(ethylene oxide)$_4$-maleimide cross-linker (DBCO-PEG$_4$-Mal; Sigma-Aldrich, 760676) by adding 4 equivalents of a 10 mM solution in dimethyl sulfoxide of the DBCO-PEG$_4$-Mal cross-linker to a ~10 μM solution of the protein in 20 mM tris, 150 mM NaCl, and 5% glycerol (pH 7.5) and incubating at room temperature for 30 min. The *a*DT-DBCO conjugate was then purified by dialysis against tris (pH 7.5) and 1% glycerol for 48 hours to remove any excess cross-linker. The *a*DT-DBCO conjugate was characterized by absorbance to confirm a presence of a peak at 309 nm, representing the incorporation of the DBCO moiety (75% yield). The *a*DT-DBCO conjugate was then mixed with an azide-containing siRNA at a 1:1 ratio, followed by a 1-hour incubation at room temperature, overnight incubation at −20°C, and 1-hour incubation at 4°C. The conjugate was then bound to nickel beads for 1 hour at 4°C, eluted from the beads in 500 mM imidazole, and buffer-exchanged into tris (pH 7.5) and 1% glycerol. Successful conjugation was confirmed by polyacrylamide gel electrophoresis analysis, and conjugation efficiency was quantified using ImageJ software (45% total yield; 80% recovery of DT, 55% siRNA conjugation efficiency).

Gene knockdown assays—Treatment with *a*DT-siRNA conjugate

*a*DT-siRNA was mixed with Opti-MEM for a final concentration of 50 nM and added to 24-well Primaria plates coated with PLO/laminin. Cells were then added to the plates with the conjugate at a density of 50,000 cells per well. Twenty four hours following treatment, cells were collected and lysed. RNA was purified from the cells, and gene expression was analyzed via quantitative reverse transcription polymerase chain reaction (qPCR).

Gene knockdown assays—Positive control treatment with Lipofectamine RNAiMAX

Transfection complexes with Lipofectamine RNAiMAX (Thermo Fisher Scientific, 13778075) were prepared according to the manufacturer's protocol in a reverse transfection procedure. Briefly, siRNA and Lipofectamine were mixed in Opti-MEM serum reduced media (Thermo Fisher Scientific, 31985062) and added to 24-well Primaria plates (Corning, 353847) coated with PLO/laminin. Cells were then added to the plates with the treatment at a density of 150,000 cells per well. Twenty four hours following transfection, cells were collected and lysed. RNA was purified from the cells, and gene expression was analyzed via qPCR.

Invasion assay

Hydrogels were synthesized as previously described by Tam *et al.* (*31*) with the following modifications: 1% w/v hyaluronan-methyl furan, 2.3 mM matrix metalloproteinase–cleavable cross-linker, and 400 μM fibronectin-derived peptide with sequence Mal-SKAGPHSRNGRGDSPG. Cells were plated on hydrogels at a density of 3500 cells per hydrogel and allowed to adhere for 24 hour. Cells were then treated with *a*DT-ITGB1 conjugates at a concentration of approximately 50 nM. Forty-eight hours after treatment, fresh medium was added to each

well, and cells were fixed with 4% PFA 4 to 5 days after treatment. Cells were stained with Hoechst to identify cell nuclei, and 15-μm fluorescent beads were added to each well to label the surface of the hydrogel. Hydrogels were imaged using confocal microscopy, taking images every 20 μm on the *z* axis, and depth of invasion was analyzed using a custom MATLAB script. Normalized invasion depth was determined by setting the untreated control value to an average of 100% invasion so that four sets of experiments could be pooled together.

Adhesion assay

*a*DT-siRNA was mixed with Opti-MEM for a final concentration of 50 nM and added to 24-well Primaria plates coated with PLO/laminin. Cells were then added to the plates with the conjugate at a density of 50,000 cells per well. Twenty four hours after treatment, cells were lifted off the 2D plates using Accutase and replated on hydrogels at a density of 15,000 cells per hydrogel. One hour after replating on the hydrogel, cells were washed five times with phosphate-buffered saline and adhered cells were fixed with 4% PFA, stained with Hoechst, and imaged using confocal microscopy. The number of adhered cells was quantified using custom computational software.

Cell viability assays following treatment with *a*DT–eIF-3b

*a*DT–eIF-3b was mixed with Opti-MEM for the desired final concentration and then added to 96-well plates coated with PLO/laminin. Cells were then added to the plates with the conjugate at a density of 8000 cells per well. Fresh medium was added to each well 24 hours following treatment. At 48 hours, cell viability was measured via PrestoBlue viability assay and quantified as a percentage of untreated controls.

SUPPLEMENTARY MATERIALS

Supplementary material for this article is available at http://advances.sciencemag.org/cgi/content/full/6/18/eaaz4848/DC1

View/request a protocol for this paper from *Bio-protocol*.

REFERENCES AND NOTES

1. J. S. Henkel, M. R. βaldwin, J. T. βarbieri, Toxins from bacteria. *EXS* **100**, 1–29 (2010).
2. A. Auger, M. Park, F. Nitschke, L. M. Minassian, G. L. βeilhartz, β. A. Minassian, R. A. Melnyk, Efficient delivery of structurally diverse protein cargo into mammalian cells by a bacterial toxin. *Mol. Pharm.* **12**, 2962–2971 (2015).
3. G. L. βeilhartz, S. N. Sugiman-Marangos, R. A. Melnyk, Repurposing bacterial toxins for intracellular delivery of therapeutic proteins. *Biochem. Pharmacol.* **142**, 13–20 (2017).
4. A. E. Rabideau, β. L. Pentelute, Delivery of non-native cargo into mammalian cells using anthrax lethal toxin. *ACS Chem. Biol.* **11**, 1490–1501 (2016).
5. P. D. R. Dyer, T. R. Shepherd, A. S. Gollings, S. A. Shorter, M. A. M. Gorringe-Pattrick, C.-K. Tang, β. N. Cattoz, L. βaillie, P. C. Griffiths, S. C. W. Richardson, Disarmed anthrax toxin delivers antisense oligonucleotides and siRNA with high efficiency and low toxicity. *J. Control. Release* **220**, 316–328 (2015).
6. M. Zheng, W. Tao, Y. Zou, O. C. Farokhzad, β. Shi, Nanotechnology-based strategies for siRNA brain delivery for disease therapy. *Trends Biotechnol.* **36**, 562–575 (2018).
7. R. L. Kanasty, K. A. Whitehead, A. J. Vegas, D. G. Anderson, Action and reaction: The biological response to siRNA and its delivery vehicles. *Mol. Ther.* **20**, 513–524 (2012).
8. J. Wang, Z. Lu, M. G. Wientjes, J. L.-S. Au, Delivery of siRNA therapeutics: βarriers and carriers. *AAPS J.* **12**, 492–503 (2010).
9. R. Kanasty, J. R. Dorkin, A. Vegas, D. Anderson, Delivery materials for siRNA therapeutics. *Nat. Mater.* **12**, 967–977 (2013).
10. P. Lönn, A. D. Kacsinta, X.-S. Cui, A. S. Hamil, M. Kaulich, K. Gogoi, S. F. Dowdy, Enhancing endosomal escape for intracellular delivery of macromolecular biologic therapeutics. *Sci. Rep.* **6**, 32301 (2016).
11. J. Zhu, M. Qiao, Q. Wang, Y. Ye, S. βa, J. Ma, H. Hu, X. Zhao, D. Chen, Dual-responsive polyplexes with enhanced disassembly and endosomal escape for efficient delivery of siRNA. *Biomaterials* **162**, 47–59 (2018).
12. T. Zhang, Y. Huang, X. Ma, N. Gong, X. Liu, L. Liu, X. Ye, β. Hu, C. Li, J.-H. Tian, A. Magrini, J. Zhang, W. Guo, J.-F. Xing, M. βottini, X.-J. Liang, Fluorinated oligoethylenimine nanoassemblies for efficient siRNA-mediated gene silencing in serum-containing media by effective endosomal escape. *Nano Lett.* **18**, 6301–6311 (2018).
13. D. W. βartlett, H. Su, I. J. Hildebrandt, W. A. Weber, M. E. Davis, Impact of tumor-specific targeting on the biodistribution and efficacy of siRNA nanoparticles measured by multimodality *in vivo* imaging. *Proc. Natl. Acad. Sci. U.S.A.* **104**, 15549–15554 (2007).
14. S. βäumer, N. βäumer, N. Appel, L. Terheyden, J. Fremerey, S. Schelhaas, E. Wardelmann, F. βuchholz, W. E. βerdel, C. Müller-Tidow, Antibody-mediated delivery of anti-*KRAS*-siRNA *in vivo* overcomes therapy resistance in colon cancer. *Clin. Cancer Res.* **21**, 1383–1394 (2015).
15. T. Sugo, M. Terada, T. Oikawa, K. Miyata, S. Nishimura, E. Kenjo, M. Ogasawara-Shimizu, Y. Makita, S. Imaichi, S. Murata, K. Otake, K. Kikuchi, M. Teratani, Y. Masuda, T. Kamei, S. Takagahara, S. Ikeda, T. Ohtaki, H. Matsumoto, Development of antibody-siRNA conjugate targeted to cardiac and skeletal muscles. *J. Control. Release* **237**, 1–13 (2016).
16. T. L. Cuellar, D. βarnes, C. Nelson, J. Tanguay, S.-F. Yu, X. Wen, S. J. Scales, J. Gesch, D. Davis, A. van βrabant Smith, D. Leake, R. Vandlen, C. W. Siebel, Systematic evaluation of antibody-mediated siRNA delivery using an industrial platform of THIOMAβ–siRNA conjugates. *Nucleic Acids Res.* **43**, 1189–1203 (2015).
17. Y. M. Li, D. A. Vallera, W. A. Hall, Diphtheria toxin-based targeted toxin therapy for brain tumors. *J. Neurooncol* **114**, 155–164 (2013).
18. H. Liang, X. Ding, C. Zhou, Y. Zhang, M. Xu, C. Zhang, L. Xu, Knockdown of eukaryotic translation initiation factors 3β (EIF3β) inhibits proliferation and promotes apoptosis in glioblastoma cells. *Neurol. Sci.* **33**, 1057–1062 (2012).
19. L. Malric, S. Monferran, J. Gilhodes, S. βoyrie, P. Dahan, N. Skuli, J. Sesen, T. Filleron, A. Kowalski-Chauvel, E. Cohen-Jonathan Moyal, C. Toulas, A. Lemarié, Interest of integrins targeting in glioblastoma according to tumor heterogeneity and cancer stem cell paradigm: An update. *Oncotarget* **8**, 86947–86968 (2017).
20. β. G. Harder, M. R. βlomquist, J. Wang, A. J. Kim, G. F. Woodworth, J. A. Winkles, J. C. Loftus, N. L. Tran, Developments in blood-brain barrier penetrance and drug repurposing for improved treatment of glioblastoma. *Front. Oncol.* **8**, 462 (2018).
21. A. Oyagi, H. Hara, Essential roles of heparin-binding epidermal growth factor-like growth factor in the brain. *CNS Neurosci. Ther.* **18**, 803–810 (2012).
22. C. H. Shin, J. P. Robinson, J. A. Sonnen, A. E. Welker, D. X. Yu, M. W. Vanβrocklin, S. L. Holmen, HβEGF promotes gliomagenesis in the context of *Ink4a/Arf* and *Pten* loss. *Oncogene* **36**, 4610–4618 (2017).
23. X. Lan, D. J. Jörg, F. M. G. Cavalli, L. M. Richards, L. V. Nguyen, R. J. Vanner, P. Guilhamon, L. Lee, M. M. Kushida, D. Pellacani, N. I. Park, F. J. Coutinho, H. Whetstone, H. J. Selvadurai, C. Che, β. Luu, A. Carles, M. Moksa, N. Rastegar, R. Head, S. Dolma, P. Prinos, M. D. Cusimano, S. Das, M. βernstein, C. H. Arrowsmith, A. J. Mungall, R. A. Moore, Y. Ma, M. Gallo, M. Lupien, T. J. Pugh, M. D. Taylor, M. Hirst, C. J. Eaves, β. D. Simons, P. β. Dirks, Fate mapping of human glioblastoma reveals an invariant stem cell hierarchy. *Nature* **549**, 227–232 (2017).
24. L. Cheng, Q. Wu, O. A. Guryanova, Z. Huang, Q. Huang, J. N. Rich, S. βao, Elevated invasive potential of glioblastoma stem cells. *Biochem. Biophys. Res. Commun.* **406**, 643–648 (2011).
25. N. M. Snead, X. W. Wu, A. Li, Q. Cui, K. Sakurai, J. C. βurnett, J. J. Rossi, Molecular basis for improved gene silencing by Dicer substrate interfering RNA compared with other siRNA variants. *Nucleic Acids Res.* **41**, 6209–6221 (2013).
26. A. M. Pappenheimer Jr, Diphtheria toxin. *Annu. Rev. Biochem.* **46**, 69–94 (1977).
27. C. S. McKay, M. G. Finn, Click chemistry in complex mixtures: βioorthogonal bioconjugation. *Chem. Biol.* **21**, 1075–1101 (2014).
28. T. Kubo, Y. Takei, K. Mihara, K. Yanagihara, T. Seyama, Amino-modified and lipid-conjugated dicer-substrate siRNA enhances RNAi efficacy. *Bioconjug. Chem.* **23**, 164–173 (2012).
29. H. Takemoto, K. Miyata, T. Ishii, S. Hattori, S. Osawa, N. Nishiyama, K. Kataoka, Accelerated polymer–polymer click conjugation by freeze–thaw treatment. *Bioconjug. Chem.* **23**, 1503–1506 (2012).
30. G. MacLeod, D. A. βozek, N. Rajakulendran, V. Monteiro, M. Ahmadi, Z. Steinhart, M. M. Kushida, H. Yu, F. J. Coutinho, F. M. G. Cavalli, I. Restall, X. Hao, T. Hart, H. A. Luchman, S. Weiss, P. β. Dirks, S. Angers, Genome-wide CRISPR-Cas9 screens expose genetic vulnerabilities and mechanisms of temozolomide sensitivity in glioblastoma stem cells. *Cell Rep.* **27**, 971–986.e9 (2019).
31. R. Y. Tam, J. Yockell-Lelièvre, L. J. Smith, L. M. Julian, A. E. G. βaker, C. Choey, M. S. Hasim, J. Dimitroulakos, W. L. Stanford, M. S. Shoichet, Rationally designed 3D hydrogels model invasive lung diseases enabling high-content drug screening. *Adv. Mater.* **31**, e1806214 (2019).
32. M. Jackson, F. Hassiotou, A. Nowak, Glioblastoma stem-like cells: At the root of tumor recurrence and a therapeutic target. *Carcinogenesis* **36**, 177–185 (2015).

33. L. Johannes, M. Lucchino, Current challenges in delivery and cytosolic translocation of therapeutic RNAs. *Nucleic Acid Ther.* **28**, 178–193 (2018).
34. O. Leka, F. Vallese, M. Pirazzini, P. βerto, C. Montecucco, G. Zanotti, Diphtheria toxin conformational switching at acidic pH. *FEBS J.* **281**, 2115–2122 (2014).
35. K. Najjar, A. Erazo-Oliveras, J. W. Mosior, M. J. Whitlock, I. Rostane, J. M. Cinclair, J.-P. Pellois, Unlocking endosomal entrapment with supercharged arginine-rich peptides. *Bioconjug. Chem.* **28**, 2932–2941 (2017).
36. N. I. Marín-Ramos, T. Z. Thein, H.-Y. Cho, S. D. Swenson, W. Wang, A. H. Schönthal, T. C. Chen, F. M. Hofman, NEO212 inhibits migration and invasion of glioma stem cells. *Mol. Cancer Ther.* **17**, 625–637 (2018).
37. J. D. Humphries, A. βyron, M. J. Humphries, Integrin ligands at a glance. *J. Cell Sci.* **119**, 3901–3903 (2006).
38. K. Koshizuka, N. Kikkawa, T. Hanazawa, Y. Yamada, A. Okato, T. Arai, K. Katada, Y. Okamoto, N. Seki, Inhibition of integrin β1-mediated oncogenic signalling by the antitumor *microRNA*-29 family in head and neck squamous cell carcinoma. *Oncotarget* **9**, 3663–3676 (2017).
39. A. βradshaw, A. Wickremsekera, S. T. Tan, L. Peng, P. F. Davis, T. Itinteang, Cancer stem cell hierarchy in glioblastoma multiforme. *Front. Surg.* **3**, 21–21 (2016).
40. H. Wang, Y. Ru, M. Sanchez-Carbayo, X. Wang, J. S. Kieft, D. Theodorescu, Translation initiation factor eIF3b expression in human cancer and its role in tumor growth and lung colonization. *Clin. Cancer Res.* **19**, 2850–2860 (2013).
41. G. F. Deleavey, M. J. Damha, Designing chemically modified oligonucleotides for targeted gene silencing. *Chem. Biol.* **19**, 937–954 (2012).
42. Y. Wang, M. J. Cooke, N. Sachewsky, C. M. Morshead, M. S. Shoichet, βioengineered sequential growth factor delivery stimulates brain tissue regeneration after stroke. *J. Control. Release* **172**, 1–11 (2013).
43. Z. Wang, M. Wei, H. Zhang, H. Chen, S. Germana, C. A. Huang, J. C. Madsen, D. H. Sachs, Z. Wang, Diphtheria-toxin based anti-human CCR4 immunotoxin for targeting human CCR4+ cells in vivo. *Mol. Oncol.* **9**, 1458–1470 (2015).
44. M. Weaver, D. W. Laske, Transferrin receptor ligand-targeted toxin conjugate (Tf-CRM107) for therapy of malignant gliomas. *J. Neurooncol* **65**, 3–14 (2003).
45. N. I. Park, P. Guilhamon, K. Desai, R. F. McAdam, E. Langille, M. O'Connor, X. Lan, H. Whetstone, F. J. Coutinho, R. J. Vanner, E. Ling, P. Prinos, L. Lee, H. Selvadurai, G. Atwal, M. Kushida, I. D. Clarke, V. Voisin, M. D. Cusimano, M. βernstein, S. Das, G. βader, C. H. Arrowsmith, S. Angers, X. Huang, M. Lupien, P. β. Dirks, ASCL1 reorganizes chromatin to direct neuronal fate and suppress tumorigenicity of glioblastoma stem cells. *Cell Stem Cell* **21**, 209–224.e7 (2017).
46. S. Dolma, H. J. Selvadurai, X. Lan, L. Lee, M. Kushida, V. Voisin, H. Whetstone, M. So, T. Aviv, N. Park, X. Zhu, C. Xu, R. Head, K. J. Rowland, M. βernstein, I. D. Clarke, G. βader, L. Harrington, J. H. βrumell, M. Tyers, P. β. Dirks, Inhibition of dopamine receptor D4 impedes autophagic flux, proliferation, and survival of glioblastoma stem cells. *Cancer Cell* **29**, 859–873 (2016).
47. S. M. Pollard, K. Yoshikawa, I. D. Clarke, D. Danovi, S. Stricker, R. Russell, J. βayani, R. Head, M. Lee, M. βernstein, J. A. Squire, A. Smith, P. Dirks, Glioma stem cell lines expanded in adherent culture have tumor-specific phenotypes and are suitable for chemical and genetic screens. *Cell Stem Cell* **4**, 568–580 (2009).
48. S. Wagner, A. Herrmannová, D. Šikrová, L. S. Valášek, Human eIF3b and eIF3a serve as the nucleation core for the assembly of eIF3 into two interconnected modules: The yeast-like core and the octamer. *Nucleic Acids Res.* **44**, 10772–10788 (2016).
49. S. Kopp, M. Krüger, S. Feldmann, H. Oltmann, A. Schütte, β. Schmitz, J. βauer, H. Schulz, K. Saar, N. Huebner, M. Wehland, M. Z. Nassef, D. Melnik, S. Meltendorf, M. Infanger, D. Grimm, Thyroid cancer cells in space during the TEXUS-53 sounding rocket mission—The THYROID project. *Sci. Rep.* **8**, 10355–10355 (2018).

Acknowledgments: We thank the lab of P. Dirks (Hospital for Sick Children, Toronto) for providing the patient-derived GSCs. We thank M. J. Damha (McGill University) for thoughtful advice on siRNA chemistry. We thank members of the Shoichet and Melnyk labs for thoughtful review of this manuscript. **Funding:** We are grateful for funding from the Canadian Institute for Health Research (CHRP CPG-140191 and Foundation FDN-143276 to M.S.S. and Project RN292258-366017 to R.M.) and the Natural Sciences and Engineering Council of Canada (CHRP CHRPJ-478471-15 and Discovery RGPIN-2019-06933 to M.S.S., CGSD to A.E.A., and LCβ, PGSD to L.J.S.). M.S.S. also acknowledges salary support from the Canada Research Chairs program.
Author contributions: A.E.A. devised and performed experiments and drafted the initial manuscript. L.J.S. synthesized materials, performed experiments, and revised the manuscript. G.β. and R.M. provided materials, assisted in conceptualization and experimental design, and revised the manuscript. L.C.β. contributed to conceptualization and experimental design and revised the manuscript. E.J. assisted in performing experiments. M.S.S. provided guidance and supervision in conceptualization and experimental design and assisted in writing the manuscript. **Competing interests:** R.M. and G.β. acknowledge that the following patent is pending: R.M., A. Auger, G.β., β. Minassian, and S. Sugiman-Marangos, "Delivery of structurally diverse polypeptide cargo into mammalian cells by a bacterial toxin," PCT/CA2016/050612, priority date 1 June 2015. M.S.S. and L.J.S. acknowledge that the following patent is pending: M.S.S., W. L. Stanford, R. Y. Tam, J. Yockell-Lelièvre, and L.J.S., "Hydrogel biomimetic for invasive diseases," International PCT patent application no. PCT/CA2019/051706, priority date 29 November 2018, priority no. 62/772,807. The authors declare no other competing interests. **Data and materials availability:** All data needed to evaluate the conclusions in the paper are present in the paper and/or the Supplementary Materials. Additional data related to this paper may be requested from the authors. The *a*DT can be provided by R.M. pending scientific review and a completed material transfer agreement. Requests for the *a*DT should be submitted to R.M. The hyaluronan hydrogel can be provided by M.S.S. pending scientific review and a completed material transfer agreement. Requests for the hyaluronan hydrogel should be submitted to M.S.S.

Submitted 12 September 2019
Accepted 21 January 2020
Published 1 May 2020
10.1126/sciadv.aaz4848

Citation: A. E. Arnold, L. J. Smith, G. βeilhartz, L. C. βahlmann, E. Jameson, R. Melnyk, M. S. Shoichet, Attenuated diphtheria toxin mediates siRNA delivery. *Sci. Adv.* **6**, eaaz4848 (2020).

Science Advances

Attenuated diphtheria toxin mediates siRNA delivery

Amy E. Arnold, Laura J. Smith, Greg L. Beilhartz, Laura C. Bahlmann, Emma Jameson, Roman A. Melnyk and Molly S. Shoichet

Sci Adv **6** (18), eaaz4848.
DOI: 10.1126/sciadv.aaz4848

Science Advances (ISSN 2375-2548) is published by the American Association for the Advancement of Science, 1200 New York Avenue NW, Washington, DC 20005. The title *Science Advances* is a registered trademark of AAAS.